University of Dundee

Biochemical characterization of the initial steps of the Kennedy pathway in Trypanosoma brucei

Gibellini, Federica; Hunter, William N.; Smith, Terry K.

Citation for published version (APA):
Gibellini, F., Hunter, W. N., & Smith, T. K. (2008). Biochemical characterization of the initial steps of the Kennedy pathway in Trypanosoma brucei: the ethanolamine and choline kinases. Biochemical Journal, 415, 135-144. 10.1042/BJ20080435

Biochemical characterization of the initial steps of the Kennedy pathway in *Trypanosoma brucei*: the ethanolamine and choline kinases

Federica GIBELLINI*, William N. HUNTER* and Terry K. SMITH†[1]

*Division of Biological Chemistry and Drug Discovery, School of Life Sciences, University of Dundee, Dundee DD1 5EH, Scotland, U.K., and †Centre for Biomolecular Sciences, St Andrews University, North Haugh, St Andrews KY16 9ST, Scotland, U.K.

Ethanolamine and choline are major components of the trypanosome membrane phospholipids, in the form of GPEtn (glycerophosphoethanolamine) and GPCho (glycerophosphocholine). Ethanolamine is also found as an integral component of the GPI (glycosylphosphatidylinositol) anchor that is required for membrane attachment of cell-surface proteins, most notably the variant-surface glycoproteins. The *de novo* synthesis of GPEtn and GPCho starts with the generation of phosphoethanolamine and phosphocholine by ethanolamine and choline kinases via the Kennedy pathway. Database mining revealed two putative C/EKs (choline/ethanolamine kinases) in the *Trypanosoma brucei* genome, which were cloned, overexpressed, purified and characterized. *Tb*EK1 (*T. brucei* ethanolamine kinase 1) was shown to be catalytically active as an ethanolamine-specific kinase, i.e. it had no choline kinase activity. The K_m values for ethanolamine and ATP were found to be 18.4 ± 0.9 and 219 ± 29 μM respectively.

*Tb*C/EK2 (*T. brucei* choline/ethanolamine kinase 2), on the other hand, was found to be able to phosphorylate both ethanolamine and choline, even though choline was the preferred substrate, with a K_m 80 times lower than that of ethanolamine. The K_m values for choline, ethanolamine and ATP were 31.4 ± 2.6 μM, 2.56 ± 0.31 mM and 20.6 ± 1.96 μM respectively. Further substrate specificity analysis revealed that both *Tb*EK1 and *Tb*C/EK2 were able to tolerate various modifications at the amino group, with the exception of a quaternary amine for *Tb*EK1 (choline) and a primary amine for *Tb*C/EK2 (ethanolamine). Both enzymes recognized analogues with substituents on C-2, but substitutions on C-1 and elongations of the carbon chain were not well tolerated.

Key words: choline kinase, ethanolamine kinase, Kennedy pathway, *Trypanosoma brucei*.

INTRODUCTION

The zwitterionic glycerophospholipids GPCho (glycerophosphocholine) and GPEtn (glycerophosphoethanolamine) are the two most abundant phospholipid species in eukaryotic cells and many bacteria [1]. In the parasitic protozoan *Trypanosoma brucei*, the agent of African sleeping sickness, GPCho accounts for approximately half of all phospholipids in both life-cycle stages, whereas GPEtn forms between 16 and 21% [2]. These phospholipids contribute an important structural role to the membrane and, in addition, determine membrane fluidity and cell-surface charge. Their biosynthesis and utilization is, not surprisingly, implicated in a variety of cellular processes [1]. In mammals, GPCho is an important source of signalling molecules, and the biosynthetic intermediate PtdCho (phosphatidylcholine) has been reported to be a mitogen required for DNA synthesis induced by growth factors [3]. Owing to its physicochemical properties, GPEtn has a tendency to form non-bilayer structures, and its incorporation into membranes affects the processes of membrane trafficking and the folding, stabilization and incorporation of certain proteins into membranes [4]. Moreover, GPEtn is utilized in the biosynthesis of GPI (glycosylphosphatidylinositol), a complex glycolipid that anchors proteins to the exterior leaflet of eukaryotic plasma membranes [5–7]. This is particularly important for the bloodstream form of *T. brucei*, which expresses a dense cell-surface coat (10^7 molecules per parasite) of a GPI-anchored VSG (variant-surface glycoprotein). This coat prevents attack by components of the innate immune system and, by undergoing antigenic variation, allows the parasite to evade a specific immune response by the host.

The biosynthesis of the GPI anchor has been genetically [8–10] and chemically [11] validated as a drug target in the bloodstream form of *T. brucei*. Thus disruption of the biosynthesis of GPEtn could prevent the formation of mature GPI-anchored VSG and lead to clearance of the parasite by the host's immune system.
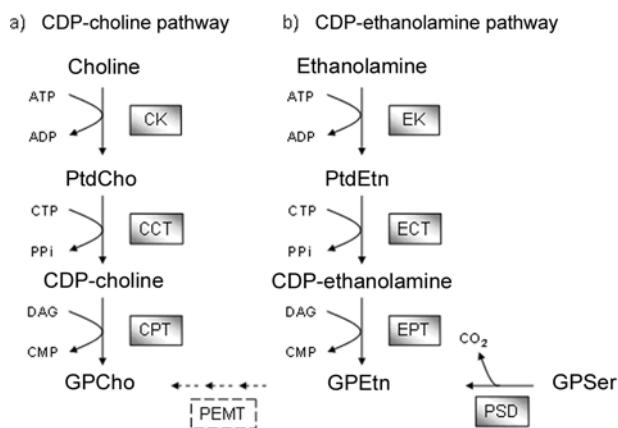
Owing to the major structural and functional roles of GPCho and GPEtn in *T. brucei*, disruption of their biosynthetic pathways is likely to interfere with the parasite biology in multiple ways and thus the enzymes involved become of interest as possible novel targets for chemotherapy. Indeed, it has been proposed that the mode of action of lysophospholipid analogues (e.g. miltefosine, edelfosine or ilmofosine) used currently against other trypanosomatid parasites, i.e. *Leishmania major*, are involved in the inhibition of GPCho biosynthesis [12].

GPEtn and GPCho are synthesized *de novo* via two branches of the same metabolic pathway, the Kennedy pathway [13] (Figure 1). Ethanolamine and choline are readily phosphorylated to generate PtdEtn (phosphatidylethanolamine) and PtdCho, which are subsequently activated to high-energy donors, CDP-ethanolamine and CDP-choline respectively, before they are coupled to diacylglycerol to form GPEtn and GPCho. For this reason, the two branches of the Kennedy pathway are often

Figure 1   Pathways for the biosynthesis of the aminoglycerophospholipids GPCho and GPEtn

The two branches of the Kennedy pathway are (**a**) the CDP-choline pathway and (**b**) the CDP-ethanolamine pathway. The relevant steps are discussed in the text. CK, choline kinase (Tb11.18.0017/Tb927.5.1140); CCT, CTP:phosphocholine cytidyltransferase (Tb10.389.0730); CPT, diacylglycerol:CDP-choline cholinephosphotransferase (Tb10.6k15.1570); EK, ethanolamine kinase (Tb11.18.0017/Tb927.5.1140); ECT, CTP:phosphoethanolamine cytidyltransferase (Tb11.01.5730); EPT, diacylglycerol:CDP-ethanolamine ethanolaminephosphotransferase (Tb10.6k15.1570); PSD, phosphatidylserine decarboxylase (Tb09.211.1610); PEMT, phosphatidylethanolamine methyltransferases; DAG, diacylglycerol. The dashed box indicates methyltransferase enzymes which are not present in either *T. brucei* or *T. cruzi*, but are present in *L. major*.

referred to as the CDP-ethanolamine or CDP-choline pathways. A second major pathway for the formation of GPEtn is via GPSer (glycerophosphoserine) decarboxylation: GPSer, which is formed through the action of a phosphatidylserine synthase, is decarboxylated by a phosphatidylserine decarboxylase to form GPEtn. In most eukaryotic cells, GPCho can also be generated from GPEtn by three methylation steps. However, according to the tritryp genomes (http://www.genedb.org), these methyltransferase genes are not present in either *T. brucei* or *Trypanosoma cruzi*, but interestingly are present in *L. major*; this has been confirmed experimentally (T.K. Smith, unpublished work).

Although the presence of the Kennedy pathway was demonstrated in *T. brucei* [14], the constituent enzymes have never been characterized. In the present paper, we report investigations into the first steps of both branches of the Kennedy pathway, involving molecular cloning, recombinant expression, purification and detailed kinetic characterization of both ethanolamine and choline kinases (EK and CK respectively) from *T. brucei*.

EXPERIMENTAL

Organisms and reagents

T. brucei strain 427 was used as a source of genomic DNA. *Escherichia coli* strains DH5α, XL-1 blue and TOP10 (Invitrogen) competent cells were used for routine manipulation, and strain BL21-Gold(DE3) (Novagen) for protein overexpression. All chemicals were purchased from either Sigma–Aldrich or Fluka. Restriction endonucleases and DNA-modifying enzymes were from New England Biolabs or Promega. [2-^{3}H]Ethanolamine (50.0 Ci/mmol) and [*methyl*-^{3}H]choline (82.0 Ci/mmol) were purchased from GE Healthcare.

RNA isolation and cDNA synthesis

Total RNA was isolated from bloodstream-form *T. brucei* using the RNeasy mini kit (Qiagen). A *Tb*C/EK2 (*T. brucei* choline/

ethanolamine kinase 2)-specific cDNA was generated and amplified using a mini-exon-specific forward primer, 5′-CGCGGATC-CGAACGCTATTATTAGAACAGTTTCTGTAC-3′, in combination with an ORF (open reading frame)-specific reverse primer, 5′-CTTCTGTTCCACGGGTATAGTC -3′, specific for the sequence of *Tb*C/EK2 using the SuperScript III One step RT (reverse transcription)–PCR kit with Platinum Taq (Invitrogen). The amplified cDNAs were purified (QIAquick PCR purification kit, Qiagen), ligated into pCR®-Blunt II TOPO® (Invitrogen) and sequenced.

Cloning of the *Tb*C/EK1 gene and construction of the pET15b-*Tb*C/EK1 expression vectors

Using the *Saccharomyces cerevisiae* EK gene sequence as a query, two putative C/EK (choline/ethanolamine kinase) genes were identified in the *T. brucei* genome database (http://www.genedb.org) using tBlastN. The two putative ORFs (Tb11.18.0017 for *Tb*C/EK1, and Tb927.5.1140 for *Tb*C/EK2) together with ∼350 bp of their 5′- and 3′-UTRs (untranslated regions), were amplified from *T. brucei* strain 427 genomic DNA using Pfu DNA polymerase and the forward and reverse primers 5′-ATAAGTAAGCGGCCGCCCGCCTAAG-TTAGAAGTTGCGCT-3′ and 5′-ATAAGTAAGCGGCCGCTC-CAATAGCTCCAGGGAAGGAAAGGGACG-3′ for *Tb*C/EK1; and 5′-ATAAGTAAGCGGCCGCAAGTGCGTTGTGCAGGT-CGGCGACGGT-3′ and 5′-ATAAGTAAGCGGCCGCCGTTGG-AAGGAGGAAAACGGCCGAGG-3′ for *Tb*C/EK2. The resulting 2.1 kb (*Tb*C/EK1 and UTRs) and 3.7 kb (*Tb*C/EK2 and UTRs) fragments were cloned into pCR®-Blunt-II TOPO®. Clones were sequenced and compared with the annotated GenBank® sequences. A BamHI restriction site, internal to the *Tb*C/EK1 ORF was silenced by site-directed mutagenesis using the forward primer 5′-GTGTTGAGGGGGATAAGC-GAATCCATCGCATGGTTCAGC-3′, the reverse primer 5′-GC-TGAACCATGCGATGGATTCGCTTATCCCCCTCAACAC-3′ and the QuikChange® site-directed mutagenesis kit (Stratagene).

The *Tb*C/EK1 ORF was PCR-amplified from the TOPO® construct with Pfu polymerase using the forward and reverse primers 5′-GGAATTCCATATGATGGAGGTGGCTGTGGG-GCAC-3′ and 5′-CGCGGATCCGCGTTATGAAGATGCACTA-AACTC-3′ respectively. The amplicon was purified (QIAquick PCR purification kit; Qiagen), ligated into pCR®-Blunt II TOPO® and sequenced. Using the NdeI and BamHI restriction sites (underlined in primer sequences), the putative *Tb*C/EK1 was ligated into the expression vector pET-15b (Novagen) modified with a TEV (tobacco etch virus) protease cleavage site (in place of a thrombin cleavage site) using the same restriction sites generating the pET-15bTEV-*Tb*C/EK1 construct. The same procedure was employed to ligate the putative *Tb*C/EK2 into the same vector using the forward and reverse primers 5′-GG-AATTCCATATGATGGCATTACGACCGTTCCCG-3′ and 5′-CGCGGATCCGCGTCAGGAAAGAAGCCCCTTCTC-3′ respectively.

The D287A and D267A mutants of *Tb*C/EK1 were generated using the QuikChange® site-directed mutagenesis kit with the forward and reverse primers 5′-GGCGCACTGAAGAT-TATTGcCTTCGAGTATGCAAAACG-3′ and 5′-CGTTTTGC-ATACTCGAAGgCAATAATCTTCAGTGCGCC-3′ respectively for the D287A mutant and the forward and reverse primers 5′-GA-GTACGTGCCACAATGcCCTGCTCAGCGGC-3′ and 5′-GC-CGCTGAGCAGGgCATTGTGGCACGTACTC-3′ respectively for the D267A mutant (the lower case letters in the primers highlight the mutated bases). All DNA sequencing was performed
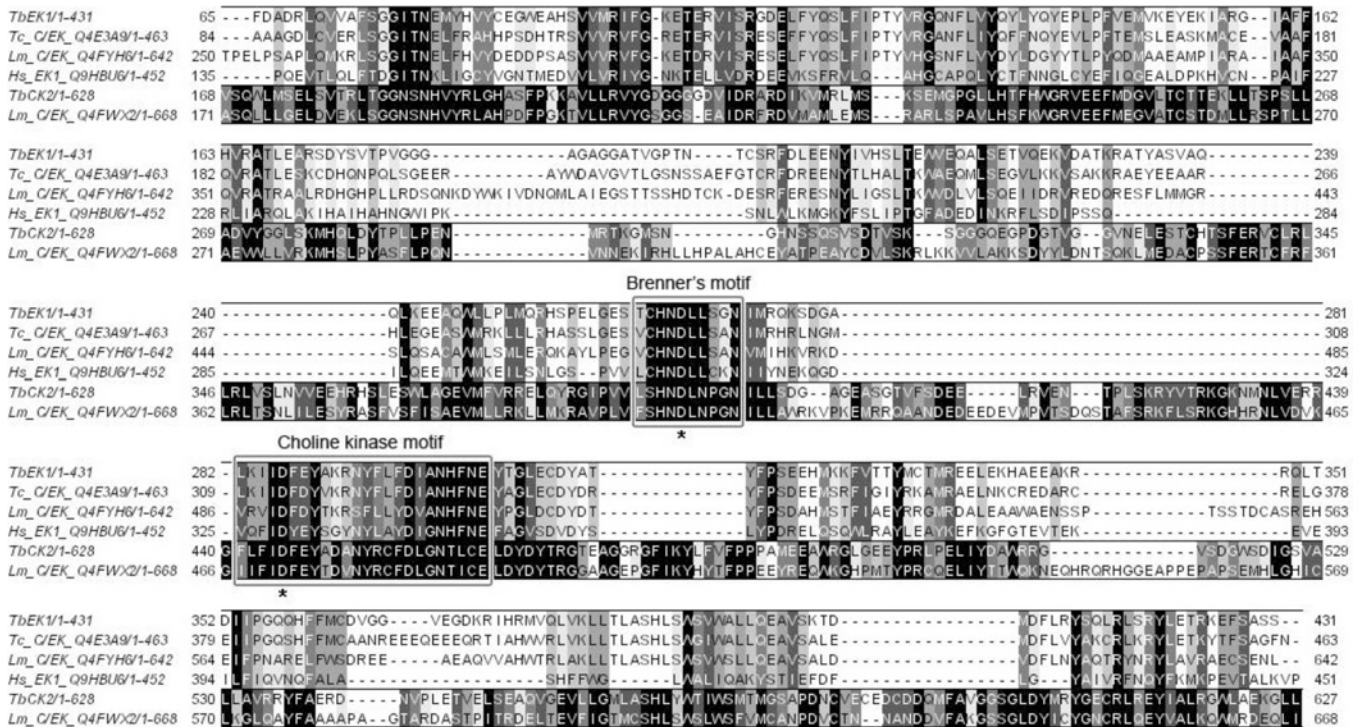
Figure 2   **A Tcoffee alignment of the predicted amino acid sequences of *Tb*EK1 (formerly *Tb*C/EK1) and *Tb*C/EK2 with CKs and EKs of other eukaryotic organisms: *T. cruzi* (Swiss-Prot accession number Q4E3A9), *L. major* (Q4FYH6 and Q4FWX2) and *Homo sapiens* (Q9HBU6)**

Residues are shaded according to percentage similarity using the Jalview 2.08.1 software. The boxes highlight the choline kinase motif and Brenner's phosphotransferase motif. The two aspartate residues marked by an asterisk were mutated in *Tb*EK1 to generate the catalytically inactive mutants D267A and D286A.

by The Sequencing Service (College of Life Sciences, University of Dundee; http://www.dnaseq.co.uk) using Applied Biosystems Big-Dye version 3.1 chemistry on an Applied Biosystems model 3730 automated capillary DNA sequencer.

Expression and purification of *Tb*C/EK1 and *Tb*C/EK2

Overproduction and sample preparation

The pET-15bTEV-*Tb*C/EK1 and the pET-15bTEV-*Tb*C/EK2 constructs were transformed in BL21-Gold(DE3) cells and clones selected on LB (Luria–Bertani) agar plates containing carbenicillin (100 μg/ml). Single colonies were grown at 37 °C in LB medium containing carbenicillin (50 μg/ml) until the D_{600} was between 0.5 and 0.7, at which point recombinant protein expression was induced with 1 mM IPTG (isopropyl β-D-thiogalactoside) and grown for 16 h at room temperature (25 °C). Cells were harvested by centrifugation at 3500 **g** for 20 min at 4 °C before being suspended in buffer A (50 mM Tris/HCl, pH 8.0, 300 mM NaCl and 10 mM imidazole). Cells were lysed in the presence of DNase I, either by sonication or using a French press, and the lysate was cleared by centrifugation at 35 000 **g** for 30 min at 4 °C.

Purification and gel filtration

The cleared lysate was applied to a 1 ml HisTrap™ FF crude column or a 5 ml HisTrap™ column (GE Healthcare) pre-loaded with Ni²⁺. Unbound proteins were removed by washing the column with 15 column vol. of buffer A, whereas *Tb*C/EK1 and *Tb*C/EK2 were eluted with an imidazole gradient in the same buffer.

Fractions containing *Tb*C/EK1 or *Tb*C/EK2 were pooled, dialysed against 50 mM Tris/HCl (pH 8) and 300 mM NaCl and purified further through a Superdex200 16/60 gel-filtration column (GE Healthcare), run in the same buffer at a rate of 1 ml/min. Low and High Molecular Weight Calibration Kits (GE Healthcare) were used to determine the molecular mass and the oligomeric state of the proteins. Purity of protein samples was assessed by SDS/PAGE (4–12 and 10 % gels) and MALDI (matrix-assisted laser-desorption ionization)–TOF (time-of-flight)-MS (Proteomics Facility, College of Life Sciences, University of Dundee).

Assay of *Tb*C/EK activity

EK or CK activity was measured by a spectrophotometric coupled assay as described previously [15]. The assay contained 50 mM Mops (pH 7.8), 150 mM KCl, 6 mM MgCl₂, 0.5 mg/ml BSA, 1 mM phosphoenolpyruvate, 0.5 mM NADH, 7 units/ml pyruvate kinase, 32 units/ml lactate dehydrogenase and 2 μg/ml *Tb*C/EK1 or 1 μg/ml *Tb*C/EK2. Concentrations of ATP and ethanolamine (or choline) were varied, and the rate of the reaction was monitored by the decrease in absorbance at 340 nm (a consequence of NADH oxidation) in a Shimadzu UV-1601 spectrophotometer. The Enzyme Kinetics module of SigmaPlot (SPSS) was used to analyse and fit the kinetic data.

The pH optimum was assessed by measuring *Tb*C/EK1 and *Tb*C/EK2 activities at various pHs: sodium acetate (pH 5.0), Bis-Tris/propane or Mops (pH 6.5), Tris/HCl (pH 7.0, 8.0 and 8.5), Mops (pH 6.0, 7.0, 7.4 and 7.8) and glycine (pH 9.0). Various ethanolamine and choline analogues were tested as substrates at least in triplicate on 96-well plates using a SpectraMAX 340PC
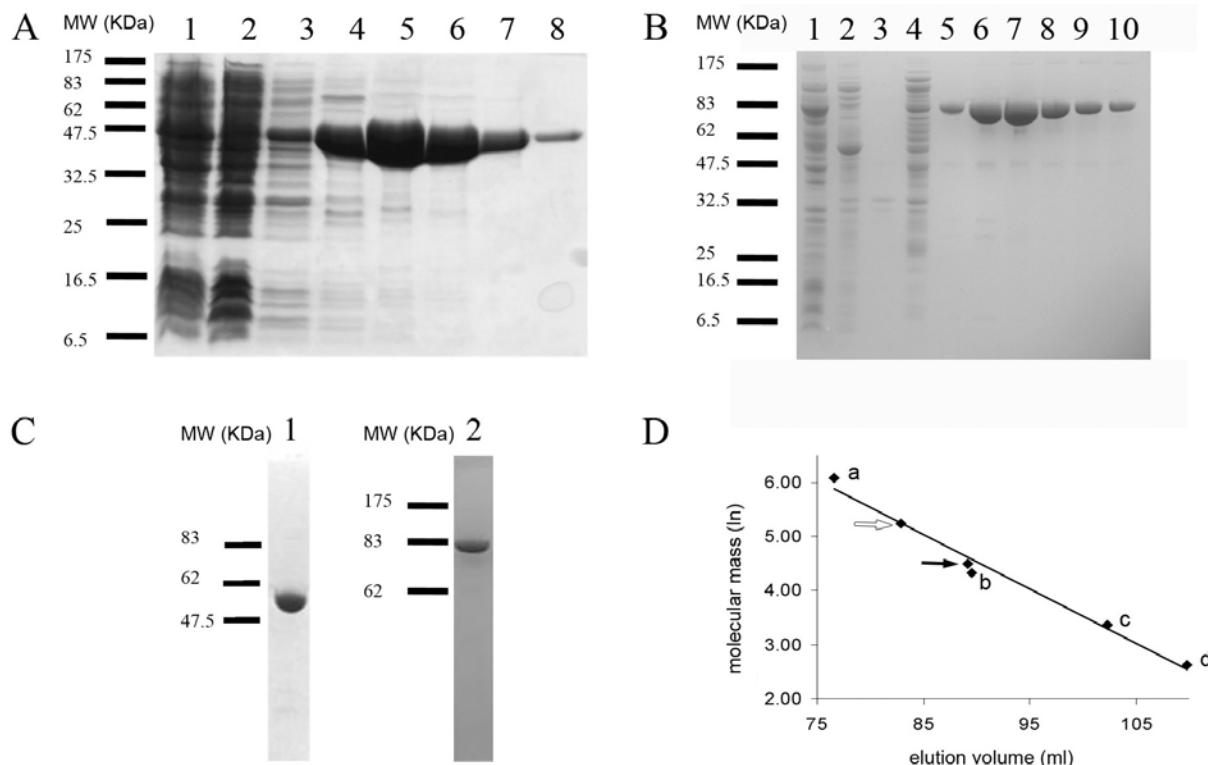
Figure 3   Expression and purification of recombinant *Tb*EK1 (formerly *Tb*C/EK1) and *Tb*C/EK2 in *E. coli*

(**A**) *Tb*EK1 protein samples from each purification step were separated by SDS/PAGE (4–12 % gel) and stained with Coomassie Brilliant Blue. Lane 1, total *E. coli* cellular protein after induction; lane 2, cleared cell lysate; lane 3, Ni^{2+} column wash at 20 mM imidazole; lane 4, Ni^{2+} column wash at 50 mM imidazole; lanes 5–8, subsequent elutions from the Ni^{2+} column at 250 mM imidazole. MW, molecular mass (in kDa). (**B**) *Tb*C/EK2 protein samples from each purification step were separated by SDS/PAGE (10 % gel) and stained with Coomassie Brilliant Blue. Lane 1, cleared *E. coli* cell lysate; lanes 2–4, washes; lanes 5–8, peak of *Tb*C/EK2 elution at 220 mM imidazole. MW, molecular mass (in kDa). (**C**) Protein samples after gel filtration separated by SDS/PAGE. Lane 1, *Tb*EK1 (4–12 % gel); lane 2, *Tb*C/EK2 (10 % gel). MW, molecular mass (in kDa). (**D**) Determination of native molecular masses of *Tb*EK1 and *Tb*C/EK2. The elution from the gel-filtration column indicates that both *Tb*EK1 (black arrow) and *Tb*C/EK2 (white arrow) are present as dimers. The following proteins were used as standards: (a) ferritin (440 kDa), (b) conalbumin (75 kDa), (c) carbonic anhydrase (29 kDa), and (d) RNase A (13.7 kDa).

plate reader (Molecular Devices), and those deemed as non-substrates were tested as inhibitors by pre-incubation at 1 mM for 5 min before the addition of ethanolamine or choline (0.1 mM).

Direct EK and CK activity assays were performed by assessing the production of PtdEtn or PtdCho, using a modified method of Kim et al. [16]. Briefly, 2 μg of purified protein was incubated with a reaction mixture (total volume of 50 μl) of 100 mM Mops (pH 7.8), 6 mM MgCl$_2$ and 5 mM ATP, with either 2 mM ethanolamine and 0.2 μCi of [^{3}H]ethanolamine or 2 mM choline and 0.2 μCi of [^{3}H]choline at 37 °C for 20 min and quenched by boiling at 100 °C for 5 min. Substrates and products were separated by HPTLC (high-performance TLC) using silica 60 plates with methanol/0.6 % NaCl/ammonium hydroxide (10:10:1, by vol.) as solvent. Radiolabelled species were detected by fluorography at −70 °C after spraying with En^{3}Hance and using Kodak XAR-5 film with an intensifying screen. Unlabelled ethanolamine and PtdEtn standards were run in parallel and visualized by spraying with ninhydrin (0.2 % in water-saturated butan-1-ol). Unlabelled PtdCho was run in parallel and visualized by iodine staining.

RESULTS AND DISCUSSION

Genomic identification and cloning of *Tb*C/EK1 and *Tb*C/EK2

Two putative C/EKs were identified in the *T. brucei* genome database (http://www.genedb.org); these putative ORFs were

PCR-amplified from genomic DNA, cloned and sequenced. Two potential initiating methionine residues were detected in the *Tb*C/EK2 ORF; this ambiguity was resolved by amplification and sequencing of the first ∼350 bp of the RT–PCR product using total RNA, a forward primer against the mini-exon and a reverse primer specific for the *Tb*C/EK2 ORF. From the cDNA sequence (Supplementary Figure S1 at http://www.BiochemJ.org/bj/415/bj4150135add.htm), the second methionine residue was identified as being the initiating residue. Interestingly, there seems to be an extra 'stuffer' sequence (65 bp) between this and the mini-exon (Supplementary Figure S1), which may represent some form of regulatory element, a concept we are currently investigating.

The predicted molecular masses of the deduced amino acid sequences are 49.1 kDa (431 amino acids) for *Tb*C/EK1 and 70.1 kDa (628 amino acids) for *Tb*C/EK2. An alignment of the translated sequences of *Tb*C/EK1 and *Tb*C/EK2 with previously characterized or putative C/EKs from other organisms (Figure 2) shows significant similarities. Even though the N-terminal region is not generally well conserved among C/EKs, the C-terminal portion contains two highly conserved regions. Brenner's motif (Figure 2) has been identified in many enzymes catalysing phosphotransfer reactions, such as protein kinases and atypical kinases (the superfamily that includes the C/EK family) [17]. The second conserved cluster (Figure 2) is found specifically in members of the C/EK family and is referred to as the choline kinase motif. Previous site-directed mutagenesis studies and structural studies in *Caenorhabditis elegans* CKα2 [18,19] and the
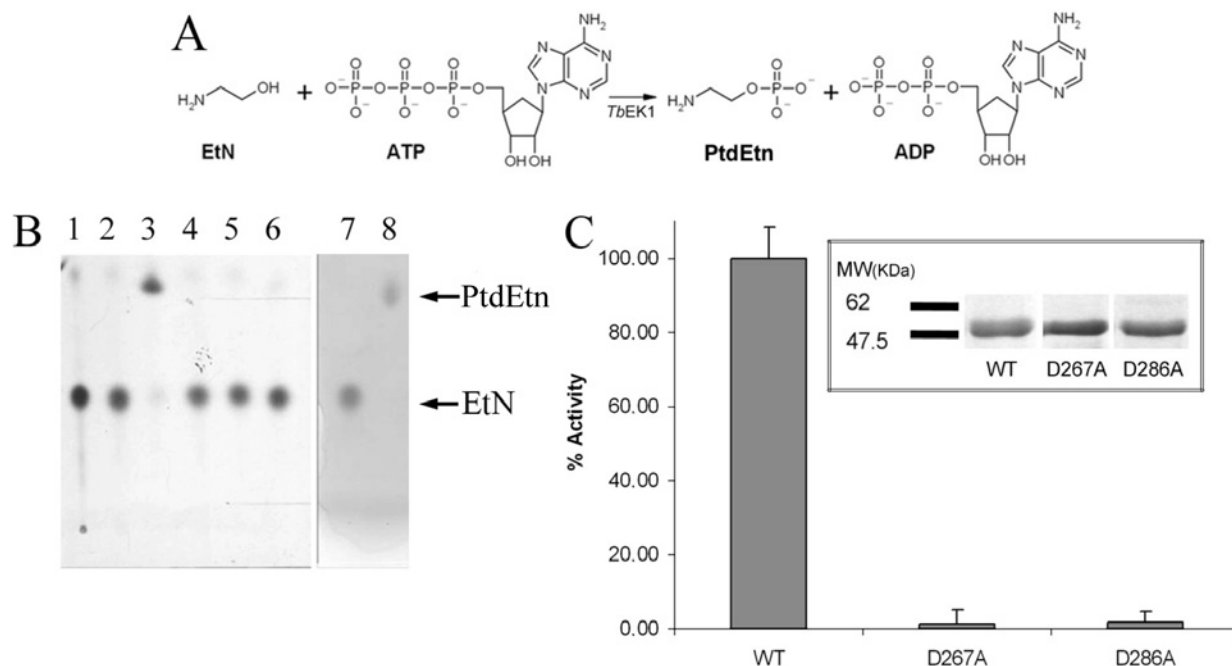
**Figure 4   Analysis of PtdEtn formation by *Tb*EK1 (formerly *Tb*C/EK1)**

(**A**) Reaction catalysed by *Tb*EK1. EtN, ethanolamine. (**B**) The substrate ethanolamine (EtN) and the product PtdEtn of the reaction were separated by HPTLC, as described in the Experimental section. Lanes 1–6, autoradiography detection. Lane 1, [^{3}H]ethanolamine standard; lane 3, standard reaction with *Tb*EK1; lanes 2 and 4, no enzyme or no Mg^{2+} added to the reaction mixture respectively (negative controls); lanes 5 and 6, standard reaction with *Tb*EK1 mutants D267A and D286A respectively; lane 7, ethanolamine standard; lane 8, PtdEtn standard detected by ninhydrin. (**C**) Enzymatic activities of wild-type (WT) *Tb*EK1 and mutants D267A and D286A assessed by spectrophotometric coupled assay as described in the Experimental section. Results are means ± S.D. ($n \geqslant 3$). The inset shows an SDS/PAGE gel of the purified proteins (wild-type and mutants). MW, molecular mass (in kDa).

Table 1   Kinetic values for recombinantly expressed and purified *Tb*EK1 (formerly *Tb*C/EK1) and *Tb*C/EK2

Results are means ± S.D. ($n \geqslant 3$).

Enzyme	V_{max} (μmol/min per mg of protein)	K_m choline (μM)	K_m ethanolamine (μM)	K_m ATP (μM)	k_{cat} (s^{-1})	k_{cat}/K_m choline (s^{-1} · mM^{-1})	k_{cat}/K_m ethanolamine (s^{-1} · mM^{-1})	k_{cat}/K_m ATP (s^{-1} · mM^{-1})
*Tb*EK1	7.62 ± 0.07	0.0 ± 0.0	18.4 ± 0.9	219.2 ± 29	6.56	–	356.53	29.93
*Tb*C/EK2	10.67 ± 0.18	31.4 ± 2.6	2560 ± 310	20.6 ± 1.96	12.91	411.25	5.04	626.86

Table 2   Substrate specificity of *Tb*EK1 (formerly *Tb*C/EK1) and *Tb*C/EK2 to utilize analogues modified at the amino group of the acceptor substrate
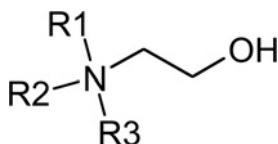
Results are means ± S.D. ($n \geqslant 3$).

R1	R2	R3	Compound	*Tb*EK1 relative rate*	*Tb*C/EK2 relative rate†
-CH$_3$	-CH$_3$	-CH$_3$	Choline	0.03 ± 1.59	100.00 ± 7.97
-H	-H	-H	Ethanolamine	100.00 ± 1.65	33.34 ± 3.34
-H	-H	-CH$_3$	*N*-Methylethanolamine	106.58 ± 9.18	135.90 ± 3.64
-H	-CH$_3$	-CH$_3$	*N,N*-Dimethylethanolamine	76.54 ± 4.86	153.33 ± 2.77
-H	-H	-CH$_2$CH$_3$	*N*-Ethylethanolamine	97.38 ± 1.59	150.57 ± 8.40
-H	-CH$_2$CH$_3$	-CH$_2$CH$_3$	*N,N*-Diethylethanolamine	47.75 ± 3.98	155.92 ± 4.32
-H	-H	-CH$_2$CH$_2$OH	Diethanolamine	88.26 ± 0.78	138.86 ± 6.30

*Analogues are compared with ethanolamine at the constant concentration of 1 mM and a saturating concentration of ATP to give a relative rate (ethanolamine = 100).
†Analogues are compared with choline at the constant concentration of 1 mM and a saturating concentration of ATP to give a relative rate (choline = 100).

analysis of the crystal structures of human CKα [20] have highlighted the importance of several of the amino acids in substrate binding. Of particular importance are the two aspartate residues marked by an asterisk in the alignment (Figure 2). These residues are involved in the binding of ATP and the stabilization of the transition state of the reaction, and their mutation leads to complete enzyme inactivation [18,20].

Not surprisingly, *Tb*C/EK1 and *Tb*C/EK2 are most closely related to C/EKs from other kinetoplastids. In the region of the alignment shown in Figure 2, *Tb*C/EK1 is 63 % identical with a putative C/EK from *T. cruzi* and *Tb*C/EK2 is 40 % identical with a putative C/EK from *L. major*. The similarity towards previously characterized C/EKs from human, yeast, *C. elegans* and *Plasmodium falciparum* is much lower (results not shown), with the exception of Brenner's and the choline kinase motifs.

### Recombinant expression and purification of *Tb*C/EK1 and *Tb*C/EK2

In order to confirm that the putative *Tb*E/CK1 and *Tb*E/CK2 are catalytically active, the two ORFs were cloned into the vector pET-15bTEV. This vector encodes an N-terminal hexahistidine epitope tag followed by a TEV protease site, which allowed purification of the recombinant proteins via Ni^{2+} ion-affinity chromatography (Figures 3A and 3B). MALDI–TOF-MS of the recombinant *Tb*C/EK1 and *Tb*C/EK2 were very close to their theoretical masses of 51655 and 72614 Da respectively. The proteins *Tb*C/EK1 and *Tb*C/EK2 were purified further by gel filtration (Figure 3C). Elution from the gel-filtration column showed that both *Tb*C/EK1 (black arrow) and *Tb*C/EK2 (white arrow) exhibited a dimeric state in solution (Figure 3D). This is similar to most of the C/EKs from other sources [21–23], with the notable exception of the monomeric *P. falciparum* CK [15]. Typical yields were 10 and 15 mg/l of bacterial culture for *Tb*C/EK1 and *Tb*C/EK2 respectively. TbC/EK1 was found to lose activity over time, being lost completely after a couple of days. It is also prone to precipitation upon freeze–thawing, and therefore assays were preformed on freshly prepared batches. TbC/EK2, on the other hand, was stable, and freeze–thawing did not lead to loss of activity or precipitation.

Kinetic analysis of *Tb*C/EK1 and *Tb*C/EK2

Previously characterized C/EKs from various sources [15,21–25] have exhibited different specificity towards the two substrates, choline and ethanolamine. It was therefore necessary to test the activity of the purified proteins in order to ascertain whether they were able to catalyse the phosphorylation of both choline and ethanolamine or if they showed selectivity to each branch of the Kennedy pathway.

*Tb*C/EK1 was found to be able to catalyse the formation of PtdEtn from ethanolamine, in an ATP- and Mg^{2+}-dependent manner (Figures 4A and 4B). However, the enzyme was unable to catalyse the formation of PtdCho from choline, in the presence of ATP and magnesium (Tables 1 and 2). This restricts the specificity of this kinase to the CDP-ethanolamine branch of the Kennedy pathway and, for this reason, *Tb*C/EK1 was renamed *Tb*EK1. To our knowledge, this is the first ethanolamine-specific kinase to be recombinantly expressed, purified to homogeneity and extensively characterized.

Kinetic analysis showed that *Tb*EK1 displayed a pH optimum at pH 8.0 (Figure 5A), with a K_m of 18.4 ± 0.9 μM for ethanolamine (Figure 5B) and a K_m of 219 ± 29 μM for ATP (Figure 5C), which is in reasonable agreement with a previously reported K_m value of 2.75 μM for EK activity from crude trypanosome homogenates [14]. The V_{max} of *Tb*EK1 is 7.62 ± 0.07 μmol/min per mg of protein, corresponding to a k_{cat} of 6.56 s^{-1} (Table 1).
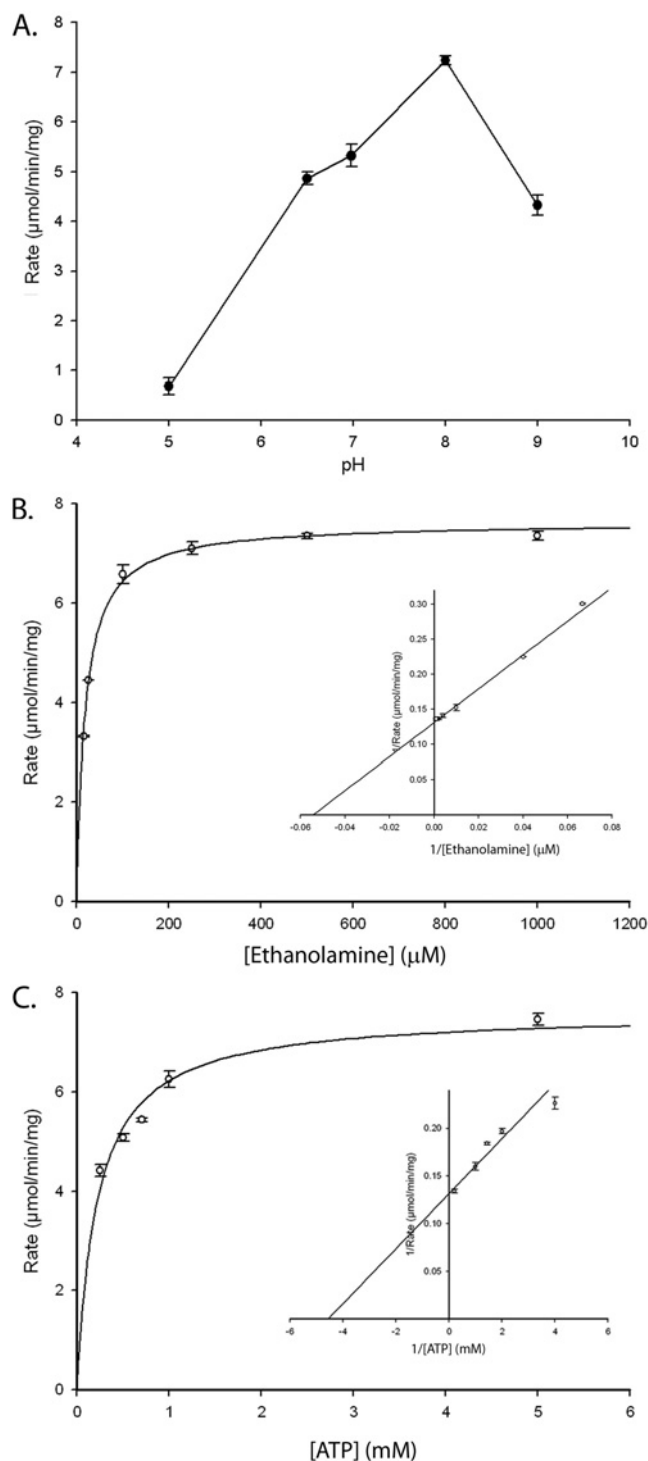
Figure 5   Kinetic analysis of *Tb*EK1 (formerly *Tb*C/EK1)

(**A**) EK activity was measured spectrophotometrically as a function of pH as described in the Experimental section. Results are means $\pm$ S.D. of three measurements. (**B**, **C**) Determination of *Tb*EK1 Michaelis–Menten constants for ethanolamine and ATP (insets are Lineweaver–Burk plots). (**B**) ATP concentration was held constant (5 mM), while ethanolamine concentration was varied. (**C**) Ethanolamine concentration was held constant (2 mM), while ATP concentration was varied.

This turnover rate/specific activity compares favourably with the previously reported activities of 346 nmol/min per mg of protein for the yeast EK [16] and 10.73 μmol/min per mg of protein for a
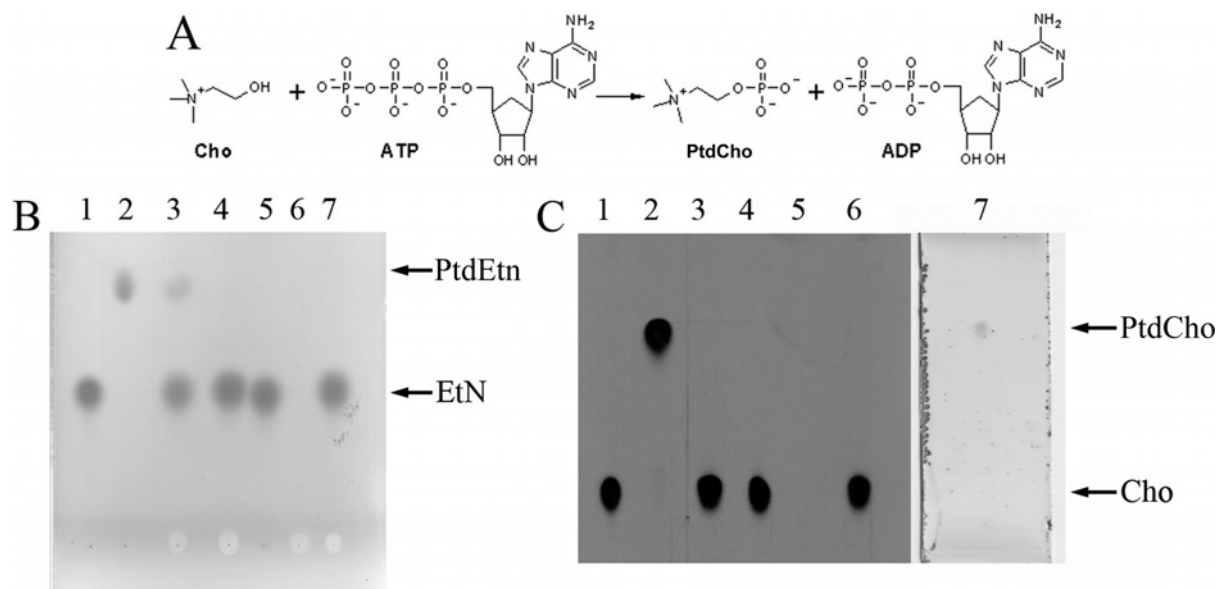
Figure 6   Analysis of PtdCho formation by *Tb*C/EK2

(**A**) Reaction catalysed by *Tb*C/EK2. Cho, choline. (**B**) The substrate ethanolamine (EtN) and the product PtdEtn of the reaction were separated by HPTLC as described in the Experimental section. Lanes 1–7, ninhydrin detection. Lane 1, ethanolamine standard; lane 2, PtdEtn standard; lane 3, standard reaction with *Tb*C/EK2; lanes 4–6, no Mg^{2+}, no ethanolamine or no ATP added to the reaction mixture respectively (negative controls). (**C**) The substrate choline (Cho) and the product PtdCho of the reaction were separated by HPTLC as described in the Experimental section. Lanes 1–6, autoradiography detection; lane 7, detection by iodine staining. Lane 1, [^{3}H]choline standard; lane 2, standard reaction with *Tb*C/EK2; lanes 3–6, no enzyme, no Mg^{2+}, no [^{3}H]-choline or no ATP added to the reaction mixture respectively (negative controls); lane 7, PtdCho standard visualized by iodine staining.

soya bean EK [25]. Two catalytically inactive mutants of *Tb*EK1 were generated by substitution of alanine for Asp^{267} and Asp^{286} (Figures 4B and 4C), thus confirming the crucial importance of these two residues in the catalytic mechanism of this kinase.

*Tb*C/EK2, on the other hand, was found to be able to phosphorylate both ethanolamine (Figure 6B) and choline (Figures 6A and 6C), even though choline was the preferred substrate (Tables 1 and 2), with a K_m 80 times lower than that of ethanolamine. *Tb*C/EK2 was also dependent upon ATP and Mg^{2+} for activity (Figures 6B and 6C) with a pH optimum of 7.8 (Figure 7A). Kinetic analysis showed that *Tb*C/EK2 displayed K_m values for choline, ethanolamine and ATP of 31.4 ± 2.6 μM, 2.56 ± 0.31 mM and 20.6 ± 1.96 μM respectively with a V_{max} of 10.67 ± 0.18 μmol/min per mg of protein and a k_{cat} of 12.91 s^{-1} (Figures 7B–7D and Table 1). This value is in the range of activities reported for other eukaryotic C/EKs, and more than ten times higher than the CK from *P. falciparum* [15].

Since the *Tb*C/EK2 K_m value for ethanolamine is several orders of magnitude higher than that of *Tb*EK1 and the fact that levels of ethanolamine in human plasma are in the micromolar range [26], one can reasonably assume that *Tb*EK1 accounts for the vast majority of the ethanolamine-phosphate formation in the trypanosome. There were no differences in the kinetics between the hexahistidine-tagged and untagged (TEV-cleaved) versions of either *Tb*EK1 or *Tb*C/EK2, thus the tagged versions were used as this decreases preparation time and increases stability, which is especially important for *Tb*EK1.

Acceptor specificity of *Tb*EK1 and *Tb*C/EK2

The ability of the two enzymes to utilize chemically modified substrates for the phosphotransfer reaction was investigated using a variety of ethanolamine and choline analogues, with modifications either at the amino or the hydroxy moieties, or with additional substituents on the two-carbon backbone. Each

analogue was compared with ethanolamine (for *Tb*EK1) or choline (for *Tb*C/EK2) at a constant substrate concentration (1 mM) and a fixed saturating concentration of ATP to give a relative rate (ethanolamine/choline = 100) (Tables 2–4).

*Tb*EK1 was able to tolerate various modifications at the amino group, including secondary and tertiary amino modifications, despite having been shown earlier not to process choline (Table 2). As shown in Table 3, single methyl and ethyl substituents on the carbon backbone at C-2 [R(−)2-aminobutan-1-ol, S(+)2-aminobutan-1-ol, R(−)2-aminopropan-1-ol and S(+)2-aminopropan-1-ol] are well tolerated, but the introduction of a second methyl group at C-2 (2-amino-2-methylpropan-1-ol) or a negatively charged carboxy group (L-serine) resulted in greatly reduced or non-detectable activity respectively. Methyl substitutions on C-1 (R(−)1-aminopropan-2-ol and S(+)1-aminopropan-2-ol) diminished the ability of the compound to act as a substrate, but to varying degrees in a stereospecific fashion. The increase of the carbon backbone length by one methylene unit (3-aminopropan-1-ol) led to a pronounced decrease in activity, whereas the increase by an ethylene unit (4-aminobutan-1-ol), eliminated substrate activity completely.

*Tb*C/EK2 was able to accept analogues modified at the amino group as substrates of the reaction; in fact, secondary and tertiary amino modifications were better than choline. Notably, of the compounds tested, ethanolamine was the poorest acceptor substrate (Table 2); these findings are in contrast with those with CK from *S. cerevisiae* [24], where *N*-methylethanolamine and *N*,*N*-dimethylethanolamine were as poor substrates as ethanolamine. Compounds with methyl and ethyl alterations on C-2 are good substrates only in the (S) configuration; R(−)2-aminobutan-1-ol and R(−)2-aminopropan-1-ol are much poorer substrates, as well as 2-amino-2-methylpropan-1-ol, which bears two methyl groups at C-2 (Table 3). A reduction of activity is seen with the elongation of the carbon chain, but it is not abolished even when increased by an ethylene unit (4-aminobutan-1-ol).
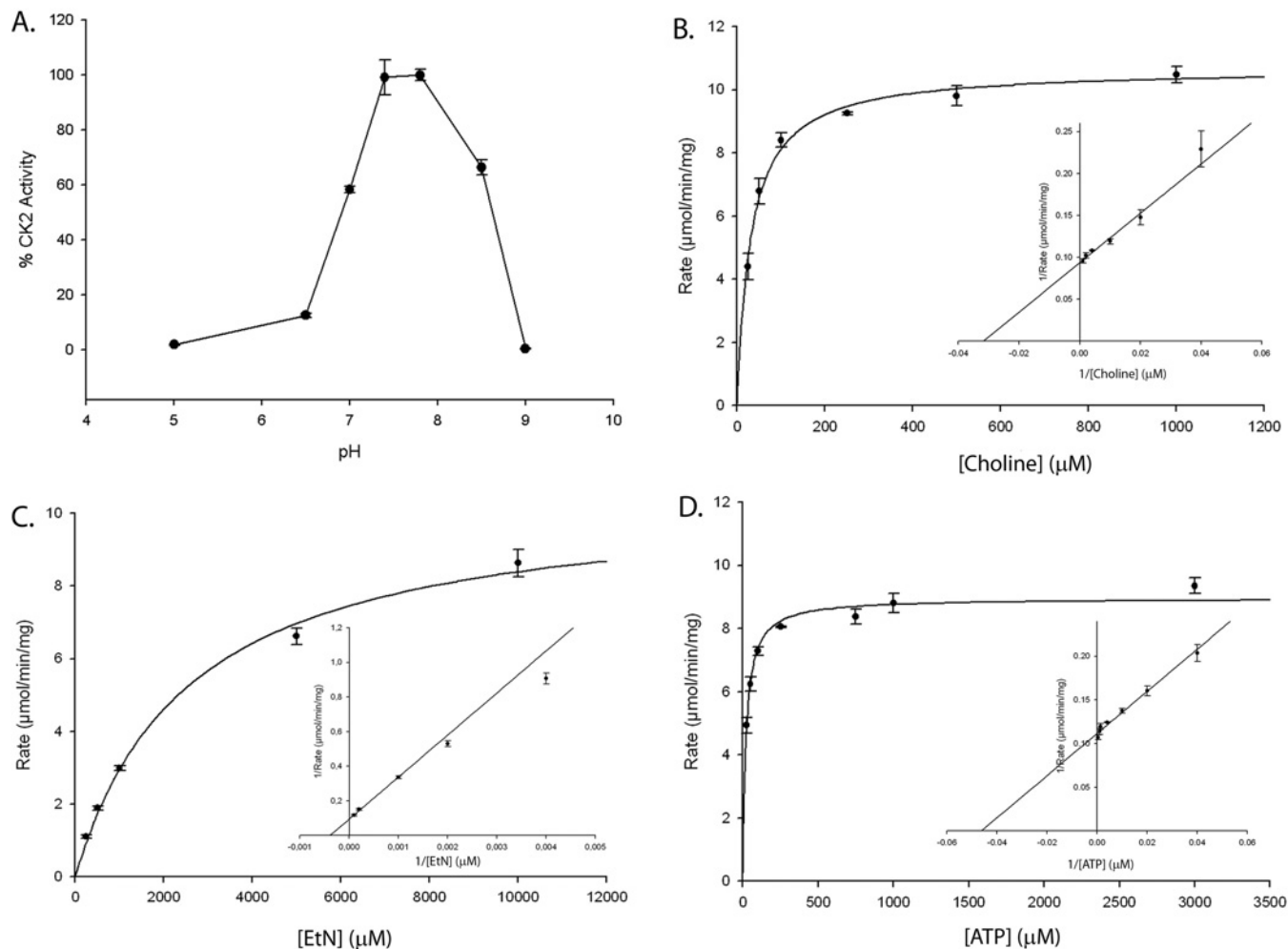
Figure 7   Kinetic analysis of *Tb*C/EK2

(**A**) CK activity was measured spectrophotometrically as a function of pH as described in the Experimental section. Results are means ± S.D. of three measurements. (**B–D**) Determination of *Tb*C/EK2 Michaelis–Menten constants for choline, ethanolamine and ATP (insets are Lineweaver–Burk plots). ATP concentration was held constant (5 mM), while choline (**B**) or ethanolamine (EtN) (**C**) concentrations were varied. (**D**) Choline concentration was held constant (2 mM), while ATP concentration was varied.

The introduction of a negative charge (L-serine), as well as the introduction of substituents at C-1 [*R*(−)1-aminopropan-2-ol and *S*(+)1-aminopropan-2-ol] are not tolerated (Table 3). That the enzyme is relatively more tolerant of substituents on C-2 is in agreement with the previous studies on the yeast orthologue [24]. As expected, modifications at the hydroxy group (Table 4) resulted in no detectable reactivity for either *Tb*EK1 or *Tb*C/EK2.

Analogues deemed as non-substrates were tested as potential inhibitors by pre-incubation at 1 mM for 5 min before the addition of ethanolamine or choline (0.1 mM) to *Tb*EK1 and *Tb*C/EK2 respectively. However, none of the potential inhibitory analogues showed any inhibitory effect (< 5 %) on either *Tb*EK1 or *Tb*C/EK2 activity.

Previous studies in *T. brucei* [14] demonstrated that ethanolamine analogues, such as *N*-methylethanolamine, *N*-ethylethanolamine, *N*,*N*-dimethylethanolamine, *S*(+)-2-aminobutan-1-ol or *R*(−)-2-aminobutan-1-ol, can be recognized by the ethanolamine transport system, whereas choline is not. There was ambiguity as to whether these compounds were acting as inhibitors of the transporter or merely competing with ethanolamine to be transported into the cell. If the latter case were true, our results suggest these analogues could be phosphorylated

by *Tb*EK1 and/or *Tb*C/EK2, and possibly proceed further in the Kennedy pathway, leading to the formation of unusual PtdEtn analogues, a concept we are currently pursuing.

Conclusions

African sleeping sickness is a neglected disease, which urgently requires new drug therapies. Characterizing fundamental differences in the biochemical pathways and enzymes therein of the parasite and its mammalian host, is an important first step towards this goal. Thus the present study represents the first identification and detailed molecular characterization of the two putative C/EKs in *T. brucei*. *Tb*EK1 is committed to only the CDP-ethanolamine branch of the Kennedy pathway since it is unable to phosphorylate choline; *Tb*C/EK2, on the other hand, was able to phosphorylate choline much more efficiently than ethanolamine. The substrate specificities for each kinase were determined, providing crucial information on the structural requirements for ligand recognition.

Analysis of the roles of *Tb*EK1 and *Tb*C/EK2 in parasite survival will be crucial to investigate their potential as drug targets for the development of new chemotherapeutic agents against

Table 3   Substrate specificity of *Tb*EK1 (formerly *Tb*C/EK1) and *Tb*C/EK2 to utilize analogues modified by extra substitutents on the carbon backbone of the acceptor substrate
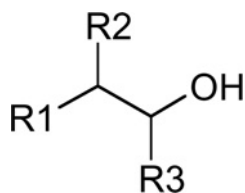
Results are means ± S.D. ($n \geqslant 3$).

R1	R2	R3	Compound	*Tb*EK1 relative rate*	*Tb*C/EK2 relative rate†
$-N^+(CH_3)_3$	-H	-H	Choline	0.03 ± 1.59	100.00 ± 7.97
$-NH_2$	-H	-H	Ethanolamine	100.00 ± 1.65	33.34 ± 3.34
$-NH_2$	$-CH_3$	-H	$R(-)$-2-Aminopropan-1-ol	107.91 ± 2.77	109.94 ± 15.42
$-NH_2$	$-CH_3$	-H	$S(+)$-2-Aminopropan-1-ol	93.75 ± 4.02	22.38 ± 1.87
$-NH_2$	$-(CH_3)_2$	-H	2-Amino-2-methylpropan-1-ol	25.58 ± 3.98	46.41 ± 6.57
$-NH_2$	$-CH_2CH_3$	-H	$S(+)$-2-Aminobutan-1-ol	114.07 ± 5.84	40.72 ± 4.93
$-NH_2$	$-CH_2CH_3$	-H	$R(-)$-2-Aminobutan-1-ol	101.74 ± 5.76	130.40 ± 9.10
$-NH_2$	$-COOH$	-H	L-Serine	0.94 ± 2.25	0.00 ± 0.00
$-NH_2$	-H	$-CH_3$	$R(-)$-1-Aminopropan-2-ol	52.41 ± 4.50	7.16 ± 0.60
$-NH_2$	-H	$-CH_3$	$S(+)$-1-Aminopropan-2-ol	6.07 ± 2.13	1.37 ± 0.15
$-CH_2NH_2$	-H	-H	3-Aminopropan-1-ol	37.52 ± 2.96	44.52 ± 4.33
$(CH_2)_2NH_2$	-H	-H	4-Aminobutan-1-ol	0.05 ± 1.93	59.95 ± 6.00

*Analogues are compared with ethanolamine at the constant concentration of 1 mM and a saturating concentration of ATP to give a relative rate (ethanolamine = 100).
†Analogues are compared with choline at the constant concentration of 1 mM and a saturating concentration of ATP to give a relative rate (choline = 100).

Table 4   Substrate specificity of *Tb*EK1 (formerly *Tb*C/EK1) and *Tb*C/EK2 to utilize analogues modified at the hydroxy group of the acceptor substrate
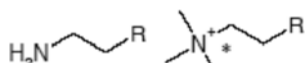
Results are means ± S.D. ($n \geqslant 3$).

R	Compound	*Tb*EK1 relative rate*	*Tb*C/EK2 relative rate†
-OH	Choline	0.03 ± 1.59	100.00 ± 7.97
-OH	Ethanolamine	100.00 ± 4.84	33.34 ± 3.34
-SH	2-Aminoethanethiol	0.01 ± 0.51	0.96 ± 0.30
$-(OCH_3)_2$	Aminoacetaldehyde dimethyl acetal	0.73 ± 0.63	0.57 ± 0.12
$-SO_3H$	Taurine	0.00 ± 0.13	0.02 ± 0.00
-H	Ethylamine	0.01 ± 0.26	0.00 ± 0.00
$-OSO_3H$	2-Aminoethyl hydrogen sulfate	0.54 ± 2.31	0.00 ± 0.00
$-OOH$	Glycine	0.35 ± 0.72	0.85 ± 0.11
$-OPO_3H_2$	Phosphoethanolamine	0.25 ± 3.32	1.35 ± 0.29
$-OCH_3$	2-Methoxyethylamine	0.00 ± 0.02	1.49 ± 0.28
$-PO_3H_2$	2-Aminoethyl phosphonic acid	0.08 ± 0.66	0.80 ± 0.18

*Analogues are compared with ethanolamine at the constant concentration of 1 mM and a saturating concentration of ATP to give a relative rate (ethanolamine = 100).
†Analogues are compared with choline at the constant concentration of 1 mM and a saturating concentration of ATP to give a relative rate (choline = 100).

African sleeping sickness and perhaps other protozoan parasites. The similarities in ligand recognition displayed by *Tb*EK1 and *Tb*C/EK2 may guide the design of inhibitors able to target both enzymes at once. Further work will characterize and assess the importance of all steps of the two branches of the Kennedy pathway, as well as their functional role(s) in the biology of the trypanosome.

REFERENCES

1 Dowhan, W. (1997) Molecular basis for membrane phospholipid diversity: why are there so many lipids? Annu. Rev. Biochem. **66**, 199–232

2 Patnaik, P. K., Field, M. C., Menon, A. K., Cross, G. A. M., Yee, M. C. and Bütikofer, P. (1993) Molecular species analysis of phospholipids from *Trypanosoma brucei* bloodstream and procyclic forms. Mol. Biochem. Parasitol. **58**, 97–105

3 Cuadrado, A., Carnero, A., Dolfi, F., Jiménez, B. and Lacal, J. C. (1993) Phosphorylcholine: a novel second messenger essential for mitogenic activity of growth factors. Oncogene **8**, 2959–2968

4 Bürgemaister, M., Birner-Grünberger, R., Heyn, M. and Daum, G. (2004) Contribution of different biosynthetic pathways to species selectivity of aminoglycerophospholipids assembled into mitochondrial membranes of the yeast *Saccharomyces cerevisiae*. Biochim. Biophys. Acta **1686**, 148–160

5 Imhof, I., Canivenc-Gansel, E., Meyer, U. and Conzelmann, A. (2000) Phosphatidylethanolamine is the donor of the phosphorylethanolamine linked to the α-1,4-linked mannose of yeast GPI structure. Glycobiology **10**, 1271–1275

6 Menon, A. K., Eppingerl, M., Mayor, S. and Schwarz, R. (1993) Phosphatidylethanolamine is the donor of the phosphoethanolamine group in trypanosome glycosyl-phosphatidylinositol. EMBO J. **12**, 1907–1914

7 Menon, A. K. and Stevens, V. L. (1992) Phosphatidylethanolamine is the donor of the ethanolamine residue linking a glycosylphosphatidylinositol anchor to protein J. Biol. Chem. **267**, 15277–15280

8 Nagamune, K., Nozaki, T., Maeda, Y., Ohishi, K., Fukuma, T., Hara, T., Schwarz, R. T., Sutterlin, C., Brun, R., Riezman, H. and Kinoshita, T. (2000) Critical roles of glycosylphosphatidylinositol for *Trypanosoma brucei*. Proc. Natl. Acad. Sci. U.S.A. **97**, 10336–10341

9 Chang, T., Milne, K. G., Guther, M. L. S., Smith, T. K. and Ferguson, M. A. J. (2002) Cloning of the *Trypanosoma brucei* and *Leishmania major* genes encoding the GlcNAc-phosphatidylinositol de-N-acetylase of biosynthesis that is essential to the African sleeping sickness parasite. J. Biol. Chem. **277**, 50176–50182

10 Ferguson, M. A. J. (2000) Glycosylphosphatidylinositol biosynthesis validated as a drug target for African sleeping sickness. Proc. Natl. Acad. Sci. U.S.A. **97**, 10673–10675

11 Smith, T. K., Crossman, A., Brimacombe, J. S. and Ferguson, M. A. J. (2004) Chemical validation of GPI biosynthesis as a drug target against African sleeping sickness. EMBO J. **23**, 4701–4708

12 Urbina, A. J. (2006) Mechanisms of action of lysophospholipid analogues against trypanosomatid parasites. Trans. R. Soc. Trop. Med. Hyg. **100**, S9–S16

13 Kennedy, E. P. and Weiss, S. B. (1956) The function of cytidine coenzymes in the biosynthesis of phospholipids. J. Biol. Chem. **222**, 193–214

14 Rifkin, M. R., Strobos, C. A. M. and Fairlamb, A. H. (1995) Specificity of ethanolamine transport and its further metabolism in *Trypanosoma brucei*. J. Biol. Chem. **270**, 16160–16166

15 Choubey, V., Guha, M., Maity, P., Kumar, S., Raghunandan, R., Maulik, P. R., Mitra, K., Halder, U. C. and Bandyopadhyay, U. (2006) Molecular characterization and localization of *Plasmodium falciparum* choline kinase. Biochim. Biophys. Acta **1760**, 1027–1038

16 Kim, K., Kim, K. H., Storey, M. K., Voelker, D. R. and Carman, G. M. (1999) Isolation and characterization of the *Saccharomyces cerevisiae EKI1* gene encoding ethanolamine kinase. J. Biol. Chem. **274**, 14857–14866

17 Scheef, E. D. and Bourne, P. E. (2005) Structural evolution of the protein kinase-like superfamily. PLoS Comput. Biol. **1**, e49

18 Yuan, C. and Kent, C. (2004) Identification of critical residues of choline kinase A2 from *Caenorhabditis elegans*. J. Biol. Chem. **276**, 17801–17809

19 Peisach, D., Gee, P., Kent, C. and Zhaohui, X. (2003) The crystal structure of choline kinase reveals a eukaryotic protein kinase fold. Structure **11**, 703–713

20 Malito, E., Sekulic, N., Cun, W., Too, S., Konrad, M. and Lavie, A. (2006) Elucidation of human choline kinase crystal structures in complex with the products ADP or phosphocholine. J. Mol. Biol. **364**, 136–151

21 Gee, P. and Kent, C., (2003) Multiple isoforms of choline kinase from *Caenorhabditis elegans*: cloning, expression, purification, and characterization. Biochim. Biophys. Acta **1648**, 33–42

22 Ayoama, C., Liao, H. and Ishidate, K. (2004) Structure and function of choline kinase isoforms in mammalian cells. Prog. Lipid Res. **43**, 266–281

23 Kim, K., Voelker, D. R., Flocco, M. T. and Carman, G. M. (1998) Expression, purification, and characterization of choline kinase, product of the *CKI* gene from *Saccharomyces cerevisiae*. J. Biol. Chem. **273**, 6844–6852

24 Clary, G. L., Tsai, C. F. and Guynn, R. W. (1986) Substrate specificity of choline kinase. Arch. Biochem. Biophys. **254**, 214–221

25 Wharfe, J. and Harwood, J. L. (1976) Lipid metabolism in germinating seeds: purification of ethanolamine kinase from soya bean. Biochim. Biophys. Acta **575**, 102–111

26 Baba, S., Watanabe, Y., Geiyo, F. and Arakawa, M. (1984) High-performance liquid chromatographic determination of serum aliphatic amines in chronic renal failure. Clin. Chim. Acta **136**, 49–56

SUPPLEMENTARY ONLINE DATA
Biochemical characterization of the initial steps of the Kennedy pathway in *Trypanosoma brucei*: the ethanolamine and choline kinases

Federica GIBELLINI*, William N. HUNTER* and Terry K. SMITH†[1]

*Division of Biological Chemistry and Drug Discovery, School of Life Sciences, University of Dundee, Dundee DD1 5EH, Scotland, U.K., and †Centre for Biomolecular Sciences, St Andrews University, North Haugh, St Andrews KY16 9ST, Scotland, U.K.

Figure S1   Sequence of cDNA of *Tb*C/EK2

Highlighted are the mini-exon sequence (grey box), the stuffer sequence (lower case) and the *Tb*C/EK2 sequence (upper case). Double-underlined is the sequence of the internal reverse primer used to generate *Tb*C/EK2 cDNA; the sequence downstream of this point is inferred from the genomic sequence.